Synthetic and Structural Studies on the Transition-Metal Fullerene Complexes $(\eta^2\text{-}C_{60})M[(\eta^5\text{-}Ph_2PC_5H_4)_2Ru]$ and $(\eta^2\text{-}C_{60})M[(\eta^5\text{-}Ph_2PC_5H_4)_2Co]^+(PF_6)^-$ (M = Pd, Pt) and the Related Compound $\{[\eta^5\text{-}Ph_2P(O)C_5H_4]_2Co\}^+(PF_6)^-$

Li-Cheng Song,* Guang-Ao Yu, Fu-Hai Su, and Qing-Mei Hu

Department of Chemistry, State Key Laboratory of Elemento-Organic Chemistry, Nankai University, Tianjin 300071, China

Received May 12, 2004

A toluene solution of C_{60} reacted with an equimolar quantity of $M(dba)_2$ (M = Pd, Pt; dba = dibenzylideneacetone) and $(\eta^5\text{-}Ph_2PC_5H_4)_2Ru$ or with $M(PPh_3)_4$ and $(\eta^5\text{-}Ph_2PC_5H_4)_2Ru$ at room temperature to give the dinuclear transition-metal fullerene complexes $(\eta^2\text{-}C_{60})M[(\eta^5\text{-}Ph_2PC_5H_4)_2Ru]$ (**1**, M = Pd; **2,** M = Pt), whereas the *o*-dichlorobenzene solution of C_{60} reacted with an equimolar amount of $M(dba)_2$ and $[(\eta^5\text{-}Ph_2PC_5H_4)_2Co]^+(PF_6)^-$ or with $M(PPh_3)_4$ and $[(\eta^5\text{-}Ph_2PC_5H_4)_2Co]^+(PF_6)^-$ under similar conditions to afford the dinuclear transition-metal fullerene complexes $(\eta^2\text{-}C_{60})M[(\eta^5\text{-}Ph_2PC_5H_4)_2Co]^+(PF_6)^-$ (**3**, M = Pd; **4,** M = Pt). In addition, the related complex $\{[\eta^5\text{-}Ph_2P(O)C_5H_4]_2Co\}^+(PF_6)^-$ (**5**) was prepared by oxidation of $[(\eta^5\text{-}Ph_2PC_5H_4)_2Co]^+(PF_6)^-$ with an excess amount of aqueous peracetic acid in acetone at room temperature. While **1**−**4** are the first examples of neutral and cationic dinuclear M/Ru and M/Co (M = Pd, Pt) fullerene complexes, **5** is the first organocobalt Cp complex containing a phosphoryl substituent. All products **1**−**5** have been fully characterized by elemental analysis, spectroscopy, and X-ray crystal diffraction techniques and, for **1** and **2**, by cyclic voltammetry.

Introduction

Transition-metal fullerene complexes are of great interest with regard to the effects of the involved metals on the chemical and physical properties of fullerenes,[1] and they may fall into two major classes. The first class includes the fullerene cores directly bonded to transition metals, such as in $(\eta^2\text{-}C_{60})Pt(PPh_3)_2$,[2] whereas the second class contains the fullerene cores indirectly bonded to transition metals, such as in $(\eta^2\text{-}C_{60})[o\text{-}(CH_2)_2C_5H_3\text{-}\eta^5]Co(\eta^4\text{-}C_4Ph_4)$.[3] Recently, we reported a series of dinuclear M/Fe (M = Pd, Pt) fullerene complexes, in which Pd or Pt is directly bonded to the C_{60} sphere and Fe is indirectly bound to the C_{60} sphere.[4] Now, as a continuation of the synthetic and structural studies of such heterodinuclear complexes, we report another series of the dinuclear M/Ru and M/Co (M = Pd, Pt) fullerene complexes $(\eta^2\text{-}C_{60})M[(\eta^5\text{-}Ph_2PC_5H_4)_2Ru]$ (**1**, M = Pd; **2**, M = Pt) and $(\eta^2\text{-}C_{60})M[(\eta^5\text{-}Ph_2PC_5H_4)_2Co]^+(PF_6)^-$ (**3**, M = Pd; **4,** M = Pt), in which Pd or Pt is directly bonded to the C_{60} cage and Ru or Co is indirectly attached to the C_{60} cage. It is worthy of note that **1**−**4** are the first neutral and ionic dinuclear M/Ru and M/Co (M = Pd, Pt) fullerene complexes, although a wide variety of transition-metal fullerene complexes are known.[5−8] We also report the first organocobalt phosphoryl containing Cp complex, $\{[\eta^5\text{-}Ph_2P(O)C_5H_4]_2Co\}^+(PF_6)^-$ (**5**), which was derived from oxidation of the

* To whom correspondence should be addressed. Fax: 0086-22-23504853. E-mail: lcsong@nankai.edu.cn.

(1) For reviews, see for example: (a) Fagan, P. J.; Calabrese, J. C.; Malone, B. *Acc. Chem. Res.* **1992**, *25*, 134. (b) Sliwa, W. *Transition Met. Chem.* **1996**, *21*, 583. (c) Balch, A. L.; Olmstead, M. M. *Chem. Rev.* **1998**, *98*, 2123. (d) Bowser, J. R. *Adv. Organomet. Chem.* **1994**, *36*, 57.

(2) Fagan, P. J.; Calabrese, J. C.; Malone, B. *Science* **1991**, *252*, 1160.

(3) Iyoda, M.; Sultana, F.; Sasaki, S.; Butenschön, H. *Tetrahedron Lett.* **1995,** *36*, 579.

(4) Song, L.-C.; Wang, G.-F.; Liu, P.-C.; Hu, Q.-M. *Organometallics* **2003**, *22*, 4593.

(5) For mononuclear fullerene derivatives, see for example: (a) Balch, A. L.; Catalano, V. J.; Lee, J. W.; Olmstead, M. M.; Parkin, S. R. *J. Am. Chem. Soc.* **1991**, *113*, 8953. (b) Balch, A. L.; Catalano, V. J.; Lee, J. W.; Olmstead, M. M. *J. Am. Chem. Soc.* **1992**, *114*, 5455. (c) Sawamura, M.; Iikura, H.; Nakamura, E. *J. Am. Chem. Soc.* **1996**, *118*, 12850. (d) Hsu, H.-F.; Du, Y.; Albrecht-Schmitt, T. E.; Wilson, S. R.; Shapley, J. R. *Organometallics* **1998**, *17*, 1756. (e) Bengough, M. N.; Thompson, D. M.; Baird, M. C.; Enright, G. D. *Organometallics* **1999**, *18*, 2950. (f) Song, L.-C.; Liu, J.-T.; Hu, Q.-M.; Weng, L.-H. *Organometallics* **2000**, *19*, 1643.

(6) For dinuclear fullerene derivatives, see for example: (a) Balch, A. L.; Lee, J. W.; Noll, B.; Olmstead, M. M. *J. Am. Chem. Soc.* **1992**, *114*, 10984. (b) Balch, A. L.; Lee, J. W.; Olmstead, M. M. *Angew. Chem., Int. Ed. Engl.* **1992**, *31*, 1356. (c) Zhang, S.; Brown, T. L.; Du, Y.; Shapley, J. R. *J. Am. Chem. Soc.* **1993**, *115*, 6705. (d) Song, L.-C.; Liu, J.-T.; Hu, Q.-M.; Wang, G.-F.; Zanello, P.; Fontani, M. *Organometallics* **2000**, *19*, 5342. (e) Mavunkal, I. J.; Chi, Y.; Peng, S.-M.; Lee, G.-H. *Organometallics* **1995**, *14*, 4454.

(7) For trinuclear fullerene derivatives, see for example: (a) Hsu, H.-F.; Shapley, J. R. *J. Am. Chem. Soc.* **1996**, *118*, 9192. (b) Park, J. T.; Song, H.; Cho, J.-J. Chung, M.-K.; Lee, J.-H.; Suh, I.-H. *Organometallics* **1998**, *17*, 227. (c) Song, H.; Lee, K.; Park, J. T.; Chio, M.-G. *Organometallics* **1998**, *17*, 4477.

(8) For multinuclear fullerene derivatives, see for example: (a) Fagan, P. J.; Calabrese, J. C.; Malone, B. *J. Am. Chem. Soc.* **1991**, *113*, 9408. (b) Balch, A. L.; Hao, L.; Olmstead, M. M. *Angew. Chem., Int. Ed. Engl.* **1996**, *35*, 188. (c) Lee, K.; Hsu, F.-F.; Shapley, J. R. *Organometallics* **1997**, *16*, 3876. (d) Lee, K.; Shapley, J. R. *Organometallics* **1998**, *17*, 3020. (e) Lee, K.; Choe, Z.-H.; Cho, Y.-J.; Song, H.; Park, J. T. *Organometallics* **2001**, *20*, 5564. (f) Lee, G.; Cho, Y.-J.; Park, B. K.; Lee, K.; Park, J. T. *J. Am. Chem. Soc.* **2003**, *125*, 13920.

10.1021/om049667a CCC: $27.50
Publication on Web 07/30/2004

Scheme 1

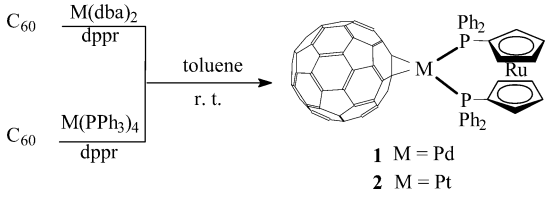

diphosphine ligand in $[(\eta^5\text{-}Ph_2PC_5H_4)_2Co]^+(PF_6)^-$, used in this paper for preparing fullerene complexes **3** and **4**.

Results and Discussion

Synthesis and Characterization of $(\eta^2\text{-}C_{60})M[(\eta^5\text{-}Ph_2PC_5H_4)_2Ru]$ (1, M = Pd; 2, M = Pt). We found that C_{60} reacted with an equimolar amount of $M(dba)_2$ (M = Pd, Pt; dba = dibenzylideneacetone) in toluene at room temperature followed by treatment of the intermediate products $(C_{60}Pd)_n$[9] and $(C_{60}Pt)_n$[10] with 1,1′-bis(diphenylphosphino)ruthenocene (dppr) to produce the transition-metal fullerene complexes **1** and **2**, whereas they could be also produced by reaction of an equimolar quantity of C_{60} with $M(PPh_3)_4$ (M = Pd, Pt) in toluene at room temperature, followed by treatment of the intermediate products $(\eta^2\text{-}C_{60})Pd(PPh_3)_2$[11] and $(\eta^2\text{-}C_{60})Pt(PPh_3)_2$[2] with the organometallic diphosphine dppr (Scheme 1).

Complexes **1** and **2** are new and have been characterized by elemental analysis, ^{1}H NMR, ^{31}P NMR, UV−vis, IR, CV, and X-ray diffraction analysis. For example, the IR spectra of **1** and **2** showed four characteristic absorption bands in the range 1434−526 cm^{-1} for their C_{60} cores,[12] whereas the ^{1}H NMR spectra of **1** and **2** each displayed one singlet at ca. 4.80 ppm for their substituted Cp rings. While the ^{31}P NMR spectrum of **1** exhibited one singlet at 21.72 ppm for its two identical P atoms, the spectrum of **2** displayed one triplet due to the ^{195}Pt−^{31}P coupling at 25.32 ppm for its two identical P atoms. The UV−vis spectra of **1** and **2** are virtually identical with each other, showing four absorption bands in the region 287−624 nm. In comparison to free C_{60}, the band at ca. 440 nm is newly generated, which suggests that the C_{60} ligand is coordinated to the Pd or Pt atom in an η^2 fashion.[13]

Although some electrochemical studies on metallofullerenes containing dppf ligands have been performed,[6d,14] no such studies on the dppr-containing metallofullerenes have been reported so far. Table 1 and Figure 1 compare the cyclic voltammetric responces exhibited by complexes **1** and **2** with that of free C_{60} in dichloromethane, at −10 °C. As can be seen from Table 1 and Figure 1, complexes **1** and **2** display three

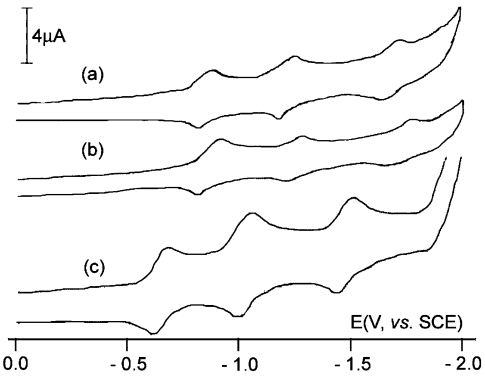

Figure 1. Cyclic voltammograms recorded at a platinum electrode in CH_2Cl_2 solutions of (a) complex **1** (0.5×10^{-3} mol dm^{-3}), (b) complex **2** (0.5×10^{-3} mol dm^{-3}), and (c) C_{60} (0.4×10^{-3} mol dm^{-3}). The supporting electrolyte was *n*-Bu_4NPF_6 (0.1 mol dm^{-3}), the scan rate was 0.2 V s^{-1}, and $T = -10$ °C.

Table 1. Formal Electrode Potentials (in V, vs SCE) and Peak-to-Peak Separations (in mV) for the Redox Changes Exhibited by the Metallofullerenes $(\eta^2\text{-}C_{60})M(dppr)$ (1, M = Pd; 2, M = Pt) and C_{60} in CH_2Cl_2 Solution at −10 °C

	fullerene-centered redns					
	$E^{\circ\prime}_{0/-}$	E_p	$E^{\circ\prime}_{-/2-}$	E_p	$E^{\circ\prime}_{2-/3-}$	E_p
1	−0.85	76	−1.22	71	−1.69	95
2	−0.86	113	−1.25	90	−1.71	85
C_{60}	−0.64	79	−1.02	73	−1.46	78

reversible or quasi-reversible fullerene-centered reductions, which are shifted by about 0.2 V toward more negative potential values with respect to the corresponding processes of free C_{60}. Such electrochemical behavior is quite similar to that previously observed for the related metallofullerenes, in which the coordinated metal fragment pushes electron density toward the fullerene ligand.[6d,14,15] Also, it can be seen that the three negative potential values of complex **1** are slightly less than the corresponding values of complex **2**. Apparently, this implies that the η^2-coordinated metal fragment Pt(dppr) in **2** is a more effective electron-pushing group than the η^2-coordinated metal fragment Pd (dppr) in **1**.

The molecular structures of **1** and **2** were unambiguously confirmed by their single-crystal X-ray studies. The molecular diagrams of **1** and **2** are shown in Figures 2 and 3, whereas Table 2 lists their selected bond lengths and angles. In fact, **1** and **2** are isostructural. While the ruthenocene diphosphine dppr ligand chelates to the Pd(1) or Pt(1) atom through its two phosphorus atoms P(1) and P(2), the C_{60} ligand coordinates to Pd(1) or Pt(1) in an η^2 fashion via its C(1)−C(2) bond between two six-membered rings. The C(1)−C(2) bond length (1.493(12) Å for **1** and 1.500(16) Å for **2**) is very close to the corresponding values observed in $(\eta^2\text{-}C_{60})Pd(dppf)$ (1.466(11) Å) and $(\eta^2\text{-}C_{60})Pt(dppf)$ (1.513(7) Å),[4] which are much longer than that of free C_{60} (1.38 Å)[16] owing to metal-to-C_{60} π-back-donation. The zerovalent Pd(1) atom in **1** or Pt(1) in **2** is at the center of a tetragon constituted by C(1), C(2), P(1), and P(2) atoms, and all

(9) Nagashima, H.; Nakaoka, A.; Saito, Y.; Kato, M.; Kawanishi, T.; Itoh, K. *J. Chem. Soc., Chem. Commun.* **1992**, 377.
(10) Nagashima, H.; Kato, Y.; Yamaguchi, H.; Kimura, E.; Kawanishi, T.; Kato, M.; Saito, Y.; Haga, M.; Itoh, K. *Chem. Lett.* **1994**, 1207.
(11) Bashilov, V. V.; Petrovskii, P. V.; Sokolov, V. I.; Lindeman, S. V.; Guzey, I. A.; Struchkov, Y. T. *Organometallics* **1993**, *12*, 991.
(12) Hare, J. P.; Dennis, T. J.; Kroto, H. W.; Taylor, R.; Allaf, A. W.; Balm, S.; Walton, D. R. M. *J. Chem. Soc., Chem. Commun.* **1991**, 412.
(13) Hirsch, A.; Grösser, T.; Skiebe, A.; Soi, A. *Chem. Ber.* **1993**, *126*, 1061.
(14) Bashilov, V. V.; Magdesieva, T. V.; Kravchuk, D. N.; Petrovskii, P. V.; Ginzburg, A. G.; Butin, K. P.; Sokolov, V. I. *J. Organomet. Chem.* **2000**, *599*, 37.
(15) Zanello, P.; Laschi, F.; Fontani, M.; Song, L.-C.; Zhu, Y.-H. *J. Organomet. Chem.* **2000**, *593*−*594*, 7.
(16) Burgi, H. B.; Blanc, E.; Schwarzenbach, D.; Liu, S.; Lu, Y.; Kappes, M. M.; Ibers, J. A. *Angew. Chem., Int. Ed. Engl.* **1992**, *31*, 640.

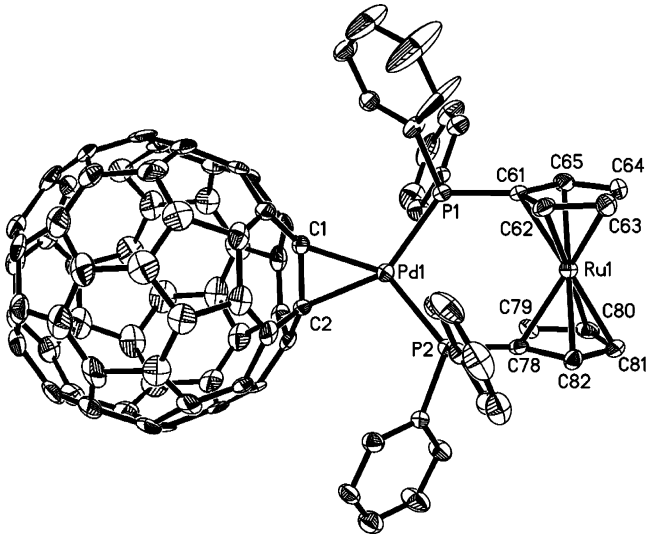

Figure 2. ORTEP diagram of **1** with ellipsoids drawn at 30% probability.

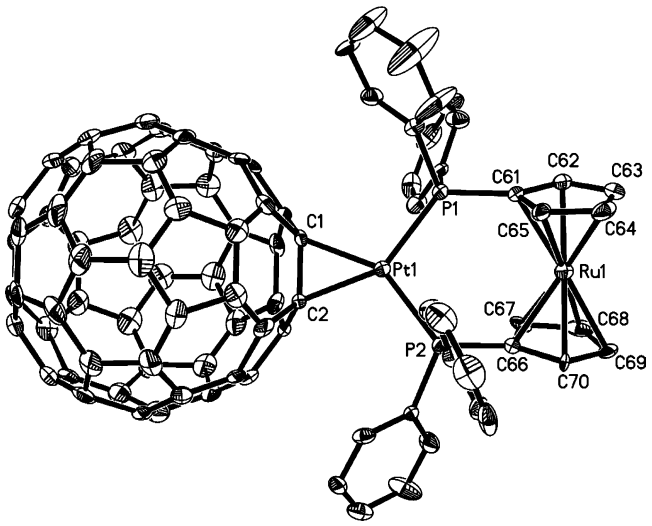

Figure 3. ORTEP diagram of **2** with ellipsoids drawn at 30% probability.

five atoms are nearly coplanar with a mean deviation of 0.0436 Å for **1** and 0.0448 Å for **2**, respectively. In addition, the two substituted Cp rings in the ruthenocene moiety of **1** or **2** (dihedral angle 4.7 or 5.7°), like those in the ferrocene unit of (η^2-C_{60})Pd(dppf) or (η^2-C_{60})Pt(dppf) (dihedral angle = 2.3° or 3.0°), are almost parallel to each other.[4] The distances between the two metal centers in **1** (Ru···Pd = 4.276 Å) and in **2** (Ru···Pt = 4.264 Å) are slightly longer than the corresponding ones in (η^2-C_{60})Pd(dppf) (Fe···Pd = 4.196 Å) and (η^2-C_{60})Pt(dppf) (Fe···Pt = 4.218 Å).[4] Thus, there are no metal−metal interactions in **1** and **2**, since such a large distance between Ru and Pd or between Ru and Pt is far greater than the sum of their van der Waals radii.

Synthesis and Characterization of (η^2-C_{60})M[(η^5-$Ph_2PC_5H_4)_2Co]^+(PF_6)^-$ (3, M = Pd; 4, M = Pt). We further found that an equimolar quantity of C_{60} reacted with $M(dba)_2$ in *o*-dichlorobenzene at room temperature, followed by treatment of the intermediate products $[C_{60}Pd]_n$[9] and $[C_{60}Pt]_n$[10] with 1,1′-bis(diphenylphosphino)-cobaltocenium hexafluorophosphate (hereafter denoted as $(dppc)^+(PF_6)^-$) or reacted with $M(PPh_3)_4$ followed by

Table 2. Selected Bond Lengths (Å) and Angles (deg) for 1 and 2

Compound **1**			
Pd(1)−C(1)	2.140(8)	C(1)−C(2)	1.493(12)
Pd(1)−C(2)	2.139(8)	C(1)−C(6)	1.500(11)
Pd(1)−P(2)	2.332(2)	C(2)−C(12)	1.462(11)
Pd(1)−P(1)	2.335(3)	Ru(1)−C(61)	2.151(8)
P(1)−C(61)	1.833(8)	Ru(1)−C(78)	2.153(8)
P(2)−C(78)	1.809(8)	C(1)−C(9)	1.453(11)
C(1)−Pd(1)−C(2)	40.8(3)	C(1)−Pd(1)−P(1)	105.5(3)
C(1)−Pd(1)−P(2)	147.5(3)	C(2)−Pd(1)−P(1)	146.0(2)
C(2)−Pd(1)−P(2)	107.1(2)	P(2)−Pd(1)−P(1)	106.89(8)
C(61)−Ru(1)−C(62)	38.7(3)	C(61)−Ru(1)−C(78)	114.3(3)
Compound **2**			
Pt(1)−C(1)	2.095(10)	C(1)−C(2)	1.500(16)
Pt(1)−C(2)	2.127(11)	C(1)−C(6)	1.524(16)
Pt(1)−P(2)	2.287(3)	C(2)−C(12)	1.442(16)
Pt(1)−P(1)	2.287(3)	Ru(1)−C(61)	2.160(11)
P(1)−C(61)	1.820(11)	Ru(1)−C(66)	2.131(12)
P(2)−C(66)	1.829(11)	C(1)−C(9)	1.464(16)
C(61)−Ru(1)−C(65)	38.4(4)	C(61)−Ru(1)−C(66)	113.4(4)
C(1)−Pt(1)−C(2)	41.6(4)	C(1)−Pt(1)−P(1)	105.3(3)
C(1)−Pt(1)−P(2)	148.1(3)	C(2)−Pt(1)−P(1)	146.6(3)
C(2)−Pt(1)−P(2)	106.8(3)	P(2)−Pt(1)−P(1)	106.46(12)

Scheme 2

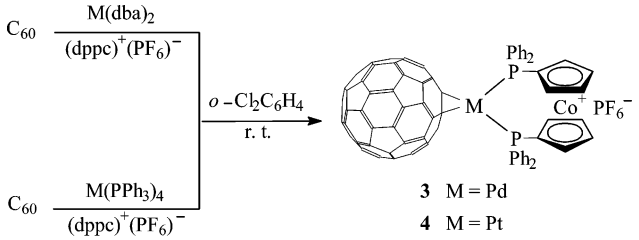

treatment of the intermediate products (η^2-C_{60})Pd-$(PPh_3)_2$[11] and (η^2-C_{60})Pt$(PPh_3)_2$[2] with $(dppc)^+(PF_6)^-$ to afford the transition-metal fullerene complexes **3** and **4** (Scheme 2).

Complexes **3** and **4** are new heterodinuclear fullerene complexes, which were fully characterized by elemental analysis, IR, ^{1}H NMR, ^{13}C NMR, ^{31}P NMR, and UV−vis spectra, as well as by X-ray diffraction analysis. The IR spectra of **3** and **4** showed four absorption bands in the range 1436−523 cm^{-1} characteristic of their C_{60} spheres,[12] while the UV−vis spectra of **3** and **4** displayed five absorption bands in the region 300−700 nm typical of their C_{60} ligands being coordinated to transition metals in an η^2 manner.[13] The ^{1}H NMR spectra of **3** and **4** showed two singlets at 5.92 and 6.07 ppm or at 5.98 and 6.08 ppm for their H^3/H^4 and H^2/H^5 protons of the substituted Cp rings, respectively. The ^{31}P NMR spectra of **3** and **4** along with that of free $(dppc)^+(PF_6)^-$ are shown in Figure 4. As can be seen in Figure 4, complex **3** diplayed one singlet at ca. 14 ppm for its two identical P atoms in the $(dppc)^+$ cation, whereas **4** exhibited one triplet at ca. 20 ppm for its two P atoms in the $(dppc)^+$ cation due to coupling between ^{195}Pt and ^{31}P (J_{Pt-P} = 3957 Hz). Either **3** or **4** showed one quintet (though theoretically a heptet) at ca. −144 ppm for its P atom in the $(PF_6)^-$ anion due to coupling between ^{31}P and ^{19}F (J_{P-F} = 711 Hz). In addition, the two P atoms of $(dppc)^+$ in free $(dppc)^+(PF_6)^-$, in contrast to those of the coordinating $(dppc)^+$ in **3** and **4**, resonated at much higher field (ca. −24 ppm), whereas the resonance signals of the P atom in the $(PF_6)^-$ anion of free $(dppc)^+(PF_6)^-$ appeared as one heptet at ca. −144 ppm, as opposed to

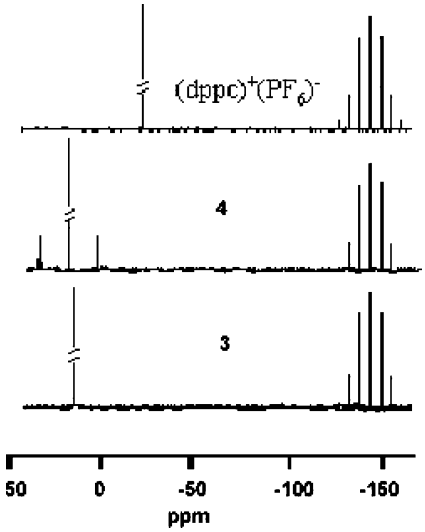

Figure 4. ^{31}P NMR spectra of complexes **3** and **4** and $(dppc)^+(PF_6)^-$.

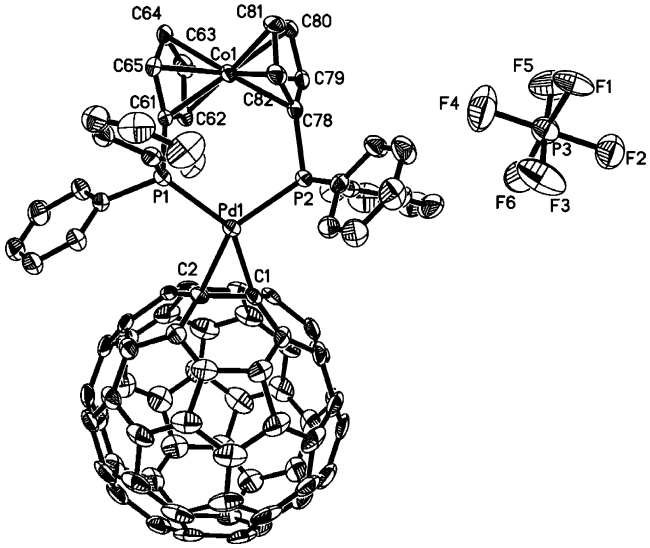

Figure 5. ORTEP diagram of **3** with ellipsoids drawn at 30% probability.

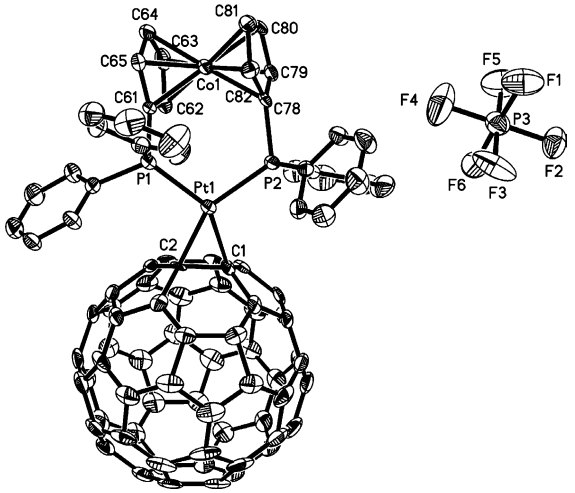

Figure 6. ORTEP diagram of **4** with ellipsoids drawn at 30% probability.

Table 3. Selected Bond Lengths (Å) and Angles (deg) for 3 and 4

		Compound **3**	
Pd(1)−C(1)	2.130(6)	C(1)−C(2)	1.459(8)
Pd(1)−C(2)	2.116(6)	C(1)−C(6)	1.462(9)
Pd(1)−P(2)	2.3080(17)	C(2)−C(12)	1.4457(9)
Pd(1)−P(1)	2.3084(19)	C(2)−C(3)	1.455(8)
P(1)−C(61)	1.812(6)	C(1)−C(9)	1.463(9)
Co(1)−C(61)	2.042(6)	Co(1)−C(78)	2.068(6)
C(1)−Pd(1)−C(2)	40.2(2)	C(1)−Pd(1)−P(1)	145.21(16)
C(1)−Pd(1)−P(2)	108.09(16)	C(2)−Pd(1)−P(1)	105.23(18)
C(2)−Pd(1)−P(2)	148.23(18)	P(2)−Pd(1)−P(1)	106.15(6)
C(61)−Co(1)−C(62)	41.1(2)	C(61)−Co(1)−C(78)	113.3(2)
		Compound **4**	
Pt(1)−C(1)	2.133(7)	C(1)−C(2)	1.494(9)
Pt(1)−C(2)	2.091(6)	C(1)−C(6)	1.4584(10)
Pt(1)−P(2)	2.2753(18)	C(2)−C(12)	1.473(10)
Pt(1)−P(1)	2.269(2)	C(2)−C(3)	1.475(10)
P(1)−C(61)	1.814(7)	C(1)−C(9)	1.482(10)
Co(1)−C(61)	2.030(6)	Co(1)−C(78)	2.065(7)
C(1)−Pt(1)−C(2)	41.4 (2)	C(1)−Pt(1)−P(1)	146.24(18)
C(1)−Pt(1)−P(2)	108.09(18)	C(2)−Pt(1)−P(1)	105.08(19)
C(2)−Pt(1)−P(2)	149.46(19)	P(2)−Pt(1)−P(1)	105.15(7)
C(61)−Co(1)−C(62)	41.3(3)	C(61)−Co(1)−C(78)	112.4(3)

a quintet for the P atom in $(PF_6)^-$ of **3** and **4**. The ^{13}C NMR spectra of **3** and **4** showed 15 and 17 signals for their C_{60} spheres, in which one signal at ca. 90 ppm can be assigned to the two C atoms attached to Pd or Pt and the others in the range 140−157 ppm to the remaining 58 C atoms of the C_{60} sphere.

The structures of **3** and **4** were unequivocally confirmed by X-ray diffraction analysis. As can be seen in Figures 5 and 6, they contain a molecule of $(dppc)^+(PF_6)^-$ chelated to Pd(1) for **1** and Pt(1) for **2** through the P(1) and P(2) atoms of the $(dppc)^+$ cation; the molecule of C_{60} is coordinated to Pd(1) for **3** and Pt(1) for **4** in an η^2 fashion through the C(1)−C(2) 6:6 bond. Table 3 shows some of their geometric parameters, which are very close to each other. Actually, **3** and **4** are also isostructural. It is noteworthy that both C(1)−C(2) 6:6 bonds in **3** and **4** are considerably longer than that in free C_{60} (1.38 Å).[16] Obviously, such elongations are due to coordination of the 6:6 bond with Pd(1) or Pt(1). In addition, the geometry around Pd(1) or Pt(1) is square planar, while the geometry of the P(3) atom in the anion $(PF_6)^-$ is octahedral. The $(dppc)^+$ ligands in **3** and **4**, similar to dppr in **1** and **2,** belong to a parallel type of sandwich structure, since the dihedral angle between the two substituted Cp rings is only 3.5° for **3** and 2.6° for **4**, respectively. It is also believed that no metal−metal interactions exist in **3** and **4**, since the distances between the two metals in **3** (Co···Pd = 4.113 Å) and in **4** (Co···Pt = 4.120 Å) are close to those in **1**, **2**, and $(\eta^2\text{-}C_{60})$M(dppf) (M = Pd, Pt)[4] and are far greater than the sum of van der Waals radii of Co and M (M = Pd, Pt).

Synthesis and Characterization of $\{[\eta^5\text{-}Ph_2P(O)C_5H_4]_2Co\}^+(PF_6)^-$ (5). Initially, we tried to obtain the C_{70} analogue of complex **3**, $(\eta^2\text{-}C_{70})Pd[(\eta^5\text{-}Ph_2PC_5H_4)_2Co]^+(PF_6)^-$, by means of the interlayer diffusion reaction process, which involves an *o*-dichlorobenzene solution of an equimolar amount of $(dppc)^+(PF_6)^-$ being diffused into a chlorobenzene solution of C_{70} and $Pd(PPh_3)_4$ for 1 week. However, it was unexpected that a very small amount of the oxidized derivative of $(dppc)^+(PF_6)^-$, namely **5**, was obtained. Apparently, the oxygen atoms in **5** originated from atmospheric O_2, because the diffusion reaction process was carried out without thorough exclusion of air. Considering that air is a very

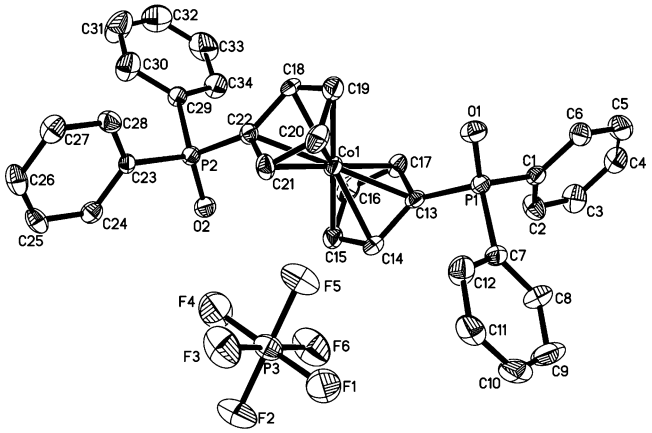

Figure 7. ORTEP diagram of **5** with ellipsoids drawn at 30% probability.

Scheme 3

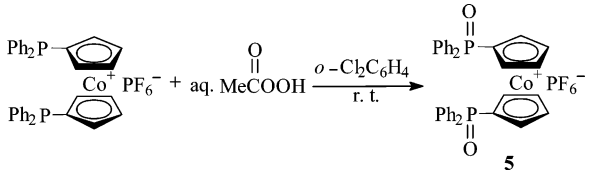

5

weak oxidant for oxidizing $(dppc)^+(PF_6)^-$ (note that $(dppc)^+(PF_6)^-$ was completely recovered after its *o*-dichlorobenzene solution was stirred in air at room temperature for 24 h), we chose a stronger oxidant, i.e., peracetic acid, to improve the yield of **5**. Fortunately, it was found that the diphosphine complex $(dppc)^+(PF_6)^-$ reacted in acetone with an excess amount of aqueous peracetic acid at room temperature for 2 h to produce **5** in nearly quantitative yield (Scheme 3).

Complex **5** is an air-stable and black crystalline solid, which has been fully characterized by elemental analysis, IR, ^{1}H NMR, ^{31}P NMR, and X-ray crystallography. For example, while the IR spectrum of **5** showed one absorption band at 1206 cm^{-1} for its P═O functionality, the ^{1}H NMR spectrum of **5** displayed two singlets at 5.98 and 6.21 ppm for H^3/H^4 and H^2/H^5 protons in its substituted Cp rings. It follows that the ^{1}H NMR signals of these Cp protons in **5** are markedly shifted toward lower field, in comparison with those of the corresponding protons in its starting material $(dppc)^+(PF_6)^-$ (two singlets at 5.59 and 5.97 ppm). Apparently, this is consistent with the substituent Ph_2P═O in **5** being a stronger electron-withdrawing group than is Ph_2P in $(dppc)^+(PF_6)^-$. The ^{31}P NMR spectrum of **5** showed one singlet at ca. 24 ppm for its P atom in the $(PF_6)^-$ anion. Therefore, the ^{31}P NMR behavior of **5** is similar to that of **3** but different from that of the free $(dppc)^+(PF_6)^-$ ligand as described above.

The molecular structure of **5** confirmed by an X-ray crystallographic study is shown in Figure 7, while its selected bond lengths and angles are given in Table 4. As can be seen in Figure 7, this molecule indeed consists of the cation $\{[\eta^5\text{-}Ph_2P(O)C_5H_4]_2Co\}^+$ and the anion $(PF_6)^-$. In fact, the structure of **5** is very similar to that of the coordinated $(dppc)^+(PF_6)^-$ in **3** and **4**. For example, (i) the two substituted Cp rings are staggered and essentially parallel with a dihedral angle of 3.5° for **3**, 2.6° for **4**, and 0.2° for **5**, (ii) the distance between the Co atom and the center of Cp ring is 1.640 Å for **3**, 1.643 Å for **4**, and 1.635 Å for **5**, and (iii) the P atom in the $(PF_6)^-$ anion of **3**, **4**, or **5** possesses an octahedral configuration with comparable P−F bond lengths and F−P−F bond angles. However, while the two $Ph_2P(O)$ substituents in the cation $\{[\eta^5\text{-}Ph_2P(O)C_5H_4]_2Co\}^+$ of **5** are trans to each other with respect to the Co metal center, the two Ph_2P substituents in the cation $\{[\eta^5\text{-}Ph_2PC_5H_4]_2Co\}^+$ of **3** or **4** are cis to each other, due to their chelation with Pd or Pt. In addition, the P═O bond lengths of P(1)−O(1) (1.459 (3) Å) and P(2)−O(2) (1.469(4) Å) are close to those reported for Ph_3P═O (1.483−1.494 Å[17]) and $[\eta^5\text{-}Ph_2P(O)C_5H_4]_2Fe\cdot 2H_2O$ (1.488 (3) Å).[18]

Table 4. Selected Bond Lengths (Å) and Angles (deg) for 5

Co(1)−C(15)	2.018(6)	P(1)−C(13)	1.811(6)
Co(1)−C(18)	2.033(5)	P(2)−O(2)	1.469(4)
P(1)−O(1)	1.459(3)	P(2)−C(22)	1.809(6)
P(1)−C(1)	1.796(6)	P(3)−F(1)	1.572(4)
C(15)−Co(1)−C(17)	68.1(3)	O(1)−P(1)−C(13)	113.0(2)
C(15)−Co(1)−C(21)	112.4(3)	O(2)−P(2)−C(22)	112.8(2)
P(1)−C(13)−Co(1)	125.3(3)	P(2)−C(22)−Co(1)	123.5(3)
O(1)−P(1)−C(1)	114.4(2)	F(2)−P(3)−F(1)	90.4(3)

Summary

We have synthesized the first dinuclear transition metal M/Ru and M/Co (M = Pd, Pt) fullerene complexes **1**−**4** and the related complex **5** in high yield. All the structures of **1**−**5** have been confirmed by X-ray diffraction crystallography as well as characterized by elemental analysis and various spectroscopic methods. While **1** and **2** are neutral fullerene complexes, **3** and **4** are ionic fullerene complexes, each containing a dinuclear metallofullerene cation and the complex anion $(PF_6)^-$. The dihedral angle between the two substituted Cp rings in the metallocene moieties of **1**−**5** is only 0.2−5.7°, which means that they still belong to parallel sandwich structural metallocenes. Through comparison of the ^{31}P NMR spectra of **3**−**5** with that of the free ligand $(dppc)^+(PF_6)^-$, it is shown that the two identical P atoms of $(dppc)^+$ in **3**−**5** are much more deshielded than those of free $(dppc)^+$, whereas the chemical shift of the P atom of $(PF_6)^-$ in **3**−**5** remains essentially the same as that of the P atom of $(PF_6)^-$ in the free ligand $(dppc)^+(PF_6)^-$. Apparently, this is because each of the two P atoms of $(dppc)^+$ in **5** is bonded to an electronegative O atom, whereas the two P atoms of $(dppc)^+$ in **3** and **4** are chelated to Pd or Pt, which is in turn attached to the electron-withdrawing C_{60} ligand. Finally, it is worth pointing out that the P-donor ligand $(dppc)^+(PF_6)^-$ has been converted to the corresponding O-donor ligand **5**, which may have uses different from the P-donor ligand in transition-metal chemistry.

Experimental Section

General Comments. All reactions were carried out under an atmosphere of highly purified nitrogen using standard Schlenk or vacuum-line techniques. While *o*-dichlorobenzene was dried with CaH_2, toluene and hexane were distilled under

(17) Gilheany, D. G. In *The Chemistry of Organophosphorus Compounds*; Hartley, F. R., Ed.; Wiley: Chichester, U.K., 1992; Vol. 2, Chapter 1, pp 9−10.

(18) Fang, Z.-G.; Hor, T. S. A.; Wen, Y. S.; Liu, L. K.; Mak, T. C. W. *Polyhedron* **1995**, *14*, 2403.

nitrogen from sodium/benzophenone ketyl. All solvents were bubbled for at least 15 min before use. C_{60} (99.9%) was available commercially. $Pd(PPh_3)_4$,[19] $Pt(PPh_3)_4$,[20] $Pd(dba)_2$,[21] $Pt(dba)_2$,[22] dppr,[23] and $(dppc)^+(PF_6)^-$ [24] were prepared according to the reported procedures. Melting points were determined on a Yanaco MP-500 melting point apparatus. Elemental analyses were performed on an Elementar Vario EL analyzer. IR and UV−vis spectra were recorded on a Bio-Rad FTS 135 and a Shimadzu TU 1901 spectrophotometer, respectively. ^{1}H NMR and ^{31}P NMR spectra were obtained on a Bruker AC-P 200 and Bruker Avance 300 spectrometer, respectively.

Preparation of (η^2-C_{60})Pd[(η^5-$Ph_2PC_5H_4)_2$Ru] (1). Method i. A 100 mL three-necked flask equipped with a magnetic stir bar, a rubber septum, and a nitrogen inlet tube was charged with 36 mg (0.05 mmol) of C_{60} and 20 mL of toluene. To the purple toluene solution of C_{60} was added 29 mg (0.05 mmol) of $Pd(dba)_2$, and then the mixture was stirred at room temperature for 0.5 h to give a black suspension. To this suspension was added 30 mg (0.05 mmol) of dppr, and the new mixture was stirred for 1 h to give a green solution. The solution was carefully layered with 60 mL of hexane. After the mixture stood for 1 day, a dark green precipitate formed, which was filtered, washed with hexane, and dried in vacuo. A 45 mg amount (63%) of **1** as a dark green crystal was obtained, mp >300 °C. Anal. Calcd for $C_{94}H_{28}P_2PdRu$: C, 79.14; H, 1.98. Found: C, 79.08; H, 1.99. IR (KBr): $\nu_{C_{60}}$ 1434 (s), 1184 (m), 579 (m), 527 (vs); ν_{Cp} 1096 (s), 1028 (m), 841 (m), 812 (s) cm^{-1}. ^{1}H NMR (200 MHz, CS_2/$CDCl_3$, TMS): δ 4.76 (s, 8H, $2C_5H_4$), 7.11−7.35 (m, 20H, $4C_6H_5$) ppm. ^{31}P NMR (81 MHz, CS_2/$CDCl_3$, H_3PO_4): δ 21.72 (s, 2P) ppm. UV−vis (C_6H_5Cl): λ_{max} (log ϵ) 289 (4.70), 334 (4.61), 443 (3.94), 624 (3.70) nm.

Method ii. The flask described above was charged with 54 mg (0.075 mmol) of C_{60} and 20 mL of toluene. To the purple solution of C_{60} was added 87 mg (0.075 mmol) of $Pd(PPh_3)_4$, and then the mixture was stirred at room temperature for 0.5 h to give a dark green solution. To this suspension was added 45 mg (0.075 mmol) of dppr, and the new mixture was stirred at room temperature for 1 h. The same workup as in method i gave 97 mg (91%) of **1**.

Preparation of (η^2-C_{60})Pt[(η^5-$Ph_2PC_5H_4)_2$Ru] (2). Method i. Similar to the preparation of **1**, when 33 mg (0.05 mmol) of $Pt(dba)_2$ was used instead of $Pd(dba)_2$, 45 mg (60%) of **2** as a dark green crystal was obtained; mp >300 °C. Anal. Calcd for $C_{94}H_{28}P_2PtRu$: C, 74.51; H, 1.86. Found: C, 74.35; H, 2.09. IR (KBr): $\nu_{C_{60}}$ 1434 (s), 1185 (m), 579 (m), 526 (vs); ν_{Cp} 1098 (s), 1028 (s), 838 (m), 810 (s) cm^{-1}. ^{1}H NMR (200 MHz, CS_2/$CDCl_3$, TMS): δ 4.81 (s, 8H, $2C_5H_4$), 7.12−7.35 (m, 20H, $4C_6H_5$) ppm. ^{31}P NMR (81 MHz, CS_2/$CDCl_3$, H_3PO_4): δ 25.32 (t, J_{P-Pt} = 4012 Hz, 2P) ppm. UV−vis (C_6H_5Cl): λ_{max} (log ϵ) 287 (4.70), 333 (4.53), 441 (3.95), 610 (3.62) nm.

Method ii. This method is similar to the preparation of **1**; when 94 mg (0.075 mmol) of $Pt(PPh_3)_4$ was used instead of $Pd(PPh_3)_4$, 105 mg (92%) of **2** was obtained.

Preparation of (η^2-C_{60})Pd[(η^5-$Ph_2PC_5H_4)_2$Co]$^+$(PF_6)$^-$ (3). Method i. This method is similar to the preparation of **1**; when 35 mg (0.05 mmol) of $(dppc)^+(PF_6)^-$ and 10 mL of *o*-dichlorobenzene were employed in place of dppr and toluene, 72 mg (94%) of **3** was obtained as a dark green solid, mp >300 °C. Anal. Calcd for $C_{94}H_{28}CoF_6P_3Pd$: C, 73.82; H, 1.85. Found: C, 73.73; H, 1.88. IR (KBr): $\nu_{C_{60}}$ 1436 (s), 1185 (m), 558 (s), 523; ν_{Cp} 1096 (s), 1028 (m), 999 (m), 840 (vs) cm^{-1}. ^{1}H NMR (200 MHz, DMSO-d_6, TMS): δ 5.92 (s, 4H, $2H^3$, $2H^4$), 6.07 (s, 4H, $2H^2$, $2H^5$), 7.18−7.85 (m, 20H, $4C_6H_5$) ppm. ^{31}P NMR (121.5 MHz, DMSO-d_6, H_3PO_4): δ 14.17 (s, 2P), −144.07 (quintet, J_{P-F} = 711 Hz, 1P) ppm. ^{13}C NMR (100.6 MHz, DMSO-d_6, TMS): δ (C_{60}) 88.76 (2C, Pd−C), 153.89 (4C, Pd−C−C), 147.19 (2C), 146.50 (2C), 145.59 (2C), 144.52 (2C), 144.22 (2C), 143.64 (4C), 143.44 (4C), 143.27 (2C), 142.70 (20C), 142.15 (4C), 141.70 (4C), 141.57 (4C), 140.89 (2C); δ $(dppc)^+$ 134.30 (4C), 133.85 (8C), 131.14 (4C), 129.46 (8C), 105.55 (2C), 86.87 (8C) ppm. UV−vis (acetone): λ_{max} (log ϵ) 324 (4.90), 332 (4.89), 438 (4.36), 613 (4.27), 659 (4.22) nm.

Method ii. This method is similar to the preparation of **1**; when 35 mg (0.05 mmol) of $(dppc)^+(PF_6)^-$ and 10 mL of *o*-dichlorobenzene were used instead of dppr and toluene, 62 mg (81%) of **3** was obtained.

Preparation of (η^2-C_{60})Pt[(η^5-$Ph_2PC_5H_4)_2$Co]$^+$(PF_6)$^-$(4). Method i. This method is similar to the preparation of **2**; when 35 mg (0.05 mmol) of $(dppc)^+(PF_6)^-$ and 10 mL of *o*-dichlorobenzene were utilized instead of dppr and toluene, 80 mg (99%) of **4** was produced as a dark green solid, mp >300 °C. Anal. Calcd for $C_{94}H_{28}CoF_6P_3Pt$: C, 69.77; H, 1.74. Found: C, 69.82; H, 1.64. IR (KBr): $\nu_{C_{60}}$ 1436 (s), 1184 (m), 558 (s), 527 (vs); ν_{Cp} 1098 (s), 1029 (m), 999 (m), 839 (vs) cm^{-1}. ^{1}H NMR (200 MHz, DMSO-d_6, TMS): δ 5.98 (s, 4H, $2H^3$, $2H^4$), 6.08 (s, 4H, $2H^2$, $2H^5$), 7.17−7.91 (m, 20H, $4C_6H_5$) ppm. ^{31}P NMR (121.5 MHz, DMSO-d_6, H_3PO_4): δ 20.20 (t, J = 3957 Hz, 2P), −144.08 (quintet, J_{P-F} = 711 Hz, 1P) ppm. ^{13}C NMR (100.6 MHz, DMSO-d_6, TMS): δ (C_{60}) 89.22 (2C, Pt−C), 156.48 (4C, Pt−C−C), 147.15 (4C), 145.91 (2C), 144.54 (2C), 144.30 (4C), 143.92 (2C), 143.81 (4C), 143.58 (4C), 143.19 (2C), 142.74 (5C), 142.64 (4C), 142.44 (5C), 141.83 (4C), 141.55 (4C), 141.33(4C), 140.25 (4C); δ $(dppc)^+$ 134.86 (4C), 133.69(8C), 131.09 (4C), 129.27 (8C), 105.00 (2C), 87.19 (8C) ppm. UV−vis (acetone): λ_{max} (log ϵ) 323 (4.75), 331 (4.75), 437 (4.20), 602 (4.01), 640 (3.94) nm.

Method ii. This method is similar to the preparation of **2**; when 35 mg (0.05 mmol) of $(dppc)^+(PF_6)^-$ and 10 mL of *o*-dichlorobenzene were employed in place of dppr and toluene, 71 mg (88%) of **4** was obtained.

Preparation of {[η^5-$Ph_2P(O)C_5H_4]_2$Co}$^+$(PF_6)$^-$ (5). To a solution of 35 mg (0.5 mmol) of $(dppc)^+(PF_6)^-$ in 10 mL of acetone was added 3.80 mL (ca. 5 mmol) of aqueous peracetic acid freshly prepared from acetic acid and hydrogen peroxide.[25] The mixture was stirred at room temperature for 2 h, during which time the color of the mixture changed from brown-yellow to brown-red. After the solvents were removed at reduced pressure, 20 mL of H_2O and 30 mL of CH_2Cl_2 were added. The new mixture was stirred thoroughly to give an aqueous phase and a CH_2Cl_2 phase. The CH_2Cl_2 phase was separated and dried over anhydrous Na_2SO_4. Removal of Na_2SO_4 and CH_2Cl_2 gave a black residue, which was redissolved in 5 mL of CH_2Cl_2. This solution was carefully layered with 20 mL of hexane overnight to give **5** as a black crystalline solid, mp 218−220 °C. Anal. Calcd for $C_{34}H_{28}CoF_6O_2P_3$: C, 55.60; H, 3.84. Found: C, 55.78; H, 3.95. IR (KBr): $\nu_{P=O}$ 1206 (s); ν_{Cp} 1102 (m), 1040 (m), 998 (m), 839 (vs) cm^{-1}. ^{1}H NMR (200 MHz, DMSO-d_6, TMS): δ 5.98 (s, 4H, $2H^3$, $2H^4$), 6.21 (s, 4H, $2H^2$, $2H^5$), 7.59−7.82 (m, 20H, $4C_6H_5$) ppm. ^{31}P NMR (81.0 MHz, DMSO-d_6, H_3PO_4): δ 24.03 (s, 2P), −139.18 (quintet, J_{P-F} = 711 Hz, 1P) ppm.

Electrochemistry. Cyclic voltammetry measurements were performed using a BAS-100B electrochemical analyzer and were carried out in dichloromethane solution containing 0.1 mol dm^{-3} *n*-Bu_4NPF_6 using a glassy-carbon working electrode and a platinum-wire counter electrode. All the potential values are referred to the saturated calomel electrode (SCE).

An argon atmosphere was continuously maintained above the solution while the experiments were in progress. The

(19) Malatesta, L.; Angoletta, M. *J. Chem. Soc.* **1957**, 1186.
(20) Malatesta, L.; Cariello, C. *J. Chem. Soc.* **1958**, 2323.
(21) Takahashi, Y.; Ito, T.; Sakai, S.; Ishii, Y. *J. Chem. Soc. D* **1970**, 1065.
(22) Cherwinski, W. J.; Johnson, B. F. G.; Lewis, J. *J. Chem. Soc., Dalton Trans.* **1974**, 1405.
(23) Li, S.;Wei, B.; Low, P. M. N.; Lee, H. K.; Hor, T. S. A.; Xue, F.; Mak, T. C. W. *J. Chem. Soc., Dalton Trans.* **1997**, 1289.
(24) Townsend, J. M.; Reingold, I. D.; Kendall, M. C. R.; Spencer, T. A. *J. Org. Chem.* **1975**, *20*, 2976.
(25) Phillips, B.; Starcher, P. S,; Ash, B. D. *J. Org. Chem.* **1959**, *23*, 1823.

Table 5. Crystal Data and Structure Refinement Details for 1−5

	1	2	3	4	5
mol formula	$C_{94}H_{28}P_2PdRu\cdot 0.5C_6H_6\cdot 1.25H_2O$	$C_{94}H_{28}P_2PtRu\cdot 0.5C_6H_6\cdot 1.75H_2O$	$C_{94}H_{28}CoF_6P_3Pd\cdot 0.5C_6H_5Me\cdot 0.75C_6H_5Cl\cdot 0.75C_6H_4Cl_2$	$C_{94}H_{28}CoF_6P_3Pt\cdot 0.5C_6H_5Me\cdot 0.75C_6H_5Cl\cdot 0.75C_6H_4Cl_2$	$C_{34}H_{28}CoF_6O_2P_3$
mol wt	1488.15	1585.85	1770.13	1858.82	734.4
temp/K	293(2)	293(2)	293(2)	293(2)	293(2)
cryst syst	monoclinic	monoclinic	monoclinic	monoclinic	monoclinic
space group	$P2_1/c$	$P2_1/c$	$P2_1/c$	$P2_1/c$	$P2_1/n$
a/Å	14.015(4)	13.974(9)	14.747(4)	14.791(4)	12.134(3)
b/Å	24.361(7)	24.285(16)	24.155(9)	24.338(7)	10.738(3)
c/Å	19.962(6)	19.922(14)	19.768(6)	19.764(5)	24.877(7)
β/deg	99.493(7)	99.279(12)	90.541(10)	90.608(5)	103.488(6)
V/Å^3	6722(4)	6672(8)	7041(4)	7114(3)	3151.9(16)
Z	4	4	4	4	4
D_c/g cm^{-3}	1.471	1.579	1.670	1.735	1.548
scan type	$\omega-2\theta$	$\omega-2\theta$	$\omega-2\theta$	$\omega-2\theta$	$\omega-2\theta$
abs coeff/mm^{-1}	0.595	2.425	0.721	2.425	0.764
F(000)	2982	3130	3552	3680	1496
$2\theta_{max}$/deg	50	50	50	50	50.06
no. of rflns	34 270	25 827	29 373	29 808	10 971
no. of indep rflns	11 791	11 282	11 873	11 883	5558
goodness of fit on F^2	0.962	1.068	1.02	1.04	0.997
no. of data/restraints/params	11 791/102/952	11 282/150/970	11 873/1428/1325	11 883/1416/1325	5558/0/415
R	0.0730	0.0798	0.0642	0.0521	0.0733
R_w	0.1280	0.1686	0.1225	0.0957	0.1087
largest diff peak and hole/e Å^{-3}	0.703 and −0.707	3.134 and −2.712	0.707 and −0.411	1.062 and −1.279	0.573 and −0.283

glassy-carbon working electrode surface was polished with 0.05 mm alumina, sonicated in distilled water, and air-dried immediately before use.

X-ray Crystallography of 1−5. While single crystals of **1** and **2** suitable for X-ray diffraction analysis were obtained by slow diffusion of hexane into a toluene solution of **1** or **2** at room temperature, those of **5** were obtained by slow diffusion of chlorobenzene into its *o*-dichlorobenzene solution. However, in contrast to the cases for **1**, **2**, and **5**, single crystals of **3** or **4** were obtained at room temperature by an interlayer diffusion reaction process, which involves an *o*-dichlorobenzene solution of $(dppc)^+(PF_6)^-$ being diffused into a chlorobenzene solution consisting of C_{60} and $M(PPh_3)_4$ (M = Pd, Pt). Each single crystal of **1** (0.20 × 0.16 × 0.14 mm), **2** (0.25 × 0.20 × 0.10 mm), **3** (0.26 × 0.24 × 0.18 mm), **4** (0.24 × 0.20 × 0.16 mm), or **5** (0.16 × 0.12 × 0.10 mm) was glued to a glass fiber and mounted on a Bruker SMART 1000 automated diffractometer. Data were collected at room temperature, using graphite-monochromated Mo Kα radiation (λ = 0.710 73 Å) in the $\omega-2\theta$ scanning mode. An absorption correction was performed using the SADABS method. The structures were solved by direct methods using the SHELXS-97 program and refined by full-matrix least-squares techniques (SHELXL-97) on F^2. Hydrogen atoms were located by using the geometric method. All calculations were performed on a Bruker Smart computer. Details of the crystals, data collections, and structure refinements are summarized in Table 5.

Acknowledgment. We are grateful to the National Natural Science Foundation of China (No. 20172026), the State Key Laboratory of Organometallic Chemistry, and the Research Fund for the Doctoral Program of Higher Education of China for financial support of this work.

Supporting Information Available: CIF files giving all crystal data, atomic coordinates and thermal parameters, and bond lengths and angles for **1**−**5**. This material is available free of charge via the Internet at http://pubs.acs.org.

OM049667A